Inorganic Chemistry Communications 101 (2019) 69–73

Contents lists available at ScienceDirect

Inorganic Chemistry Communications

journal homepage: www.elsevier.com/locate/inoche

Short communication

Two efficient near-infrared (NIR) luminescent [Ir(CˆN)$_2$(NˆO)]-characteristic complexes with 8-hydroxyquinoline (8-Hq) as the ancillary ligand

Jiahao Guo[1], Jin Zhou[1], Guorui Fu, Yani He, Wentao Li, Xingqiang Lü*

School of Chemical Engineering, Shaanxi Key Laboratory of Degradable Medical Material, Northwest University, Xi'an, 710069, Shaanxi, China

GRAPHICAL ABSTRACT

Replaced by the large π-conjugation-induced CˆN ligand **Hdpbq**, the distinctive bathochromatic shift into a typical NIR region (λ_{em} = 786 nm) for [Ir(dpbq)$_2$(8-*q*)] (**2**) relative to that (λ_{em} = 687 nm with a shoulder at 756 nm) of [Ir(iqbt)$_2$(8-*q*)] (**1**) while relatively lower quantum efficiency Φ_{em} = 0.16 *versus* Φ_{em} = 0.05 are observed.

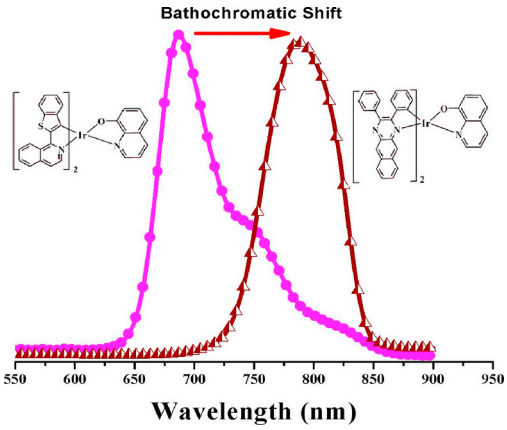

ARTICLE INFO

Keywords:
[Ir(CˆN)$_2$(NˆO)]-characteristic Ir(III)-complex
NIR luminescence
Phosphorescence
Ligands-perturbed effect

ABSTRACT

Through the utilization of **Hiqbt** (1-(benzo[*b*]-thiophen-2-yl)-isoquinoline) or **Hdpbq** (2,3-diphenyl benzo[*g*] quinoxaline) as the CˆN main ligand and **8-Hq** (8-hydroxyquinoline) as the NˆO ancillary ligand, two [Ir(CˆN)$_2$(NˆO)]-characterized heteroleptic complexes [Ir(iqbt)$_2$(8-*q*)] (**1**) and [Ir(dbpq)$_2$(8-*q*)] (**2**) with desirable soluble and NIR-phosphorescent properties (λ_{em} = 687 nm with a shoulder at 756 nm, lifetime τ = 0.73 μs and quantum efficiency Φ_{em} = 0.16 for complex **1** *versus* λ_{em} = 786 nm, lifetime τ = 0.47 μs and quantum efficiency Φ_{em} = 0.05 for complex **2**) are obtained, respectively. In comparison, the distinctive bathochromatic shift into a typical NIR region of complex **2**, arisen from the large-molecule-conjugation-induced narrow energy gap, gives rise to its relatively lower quantum efficiency than that of complex **1**.

Near-infrared (NIR) emitting materials have aroused particular interest in electroluminescent diodes promising for military optoelectronics [1], telecommunications [2] and wound healing [3]. In this perspective, although significant efforts have been devoted to inorganic NIR-emitting materials (nano-crystal [4], halide perovskite [5] or quantum dot [6], *etc*) for practical NIR-light-emitting diodes (NIR-

* Corresponding author.
E-mail address: lvxq@nwu.edu.cn (X. Lü).
[1] Both authors contributed equally.

https://doi.org/10.1016/j.inoche.2019.01.019
Received 26 December 2018; Accepted 12 January 2019
Available online 15 January 2019
1387-7003/

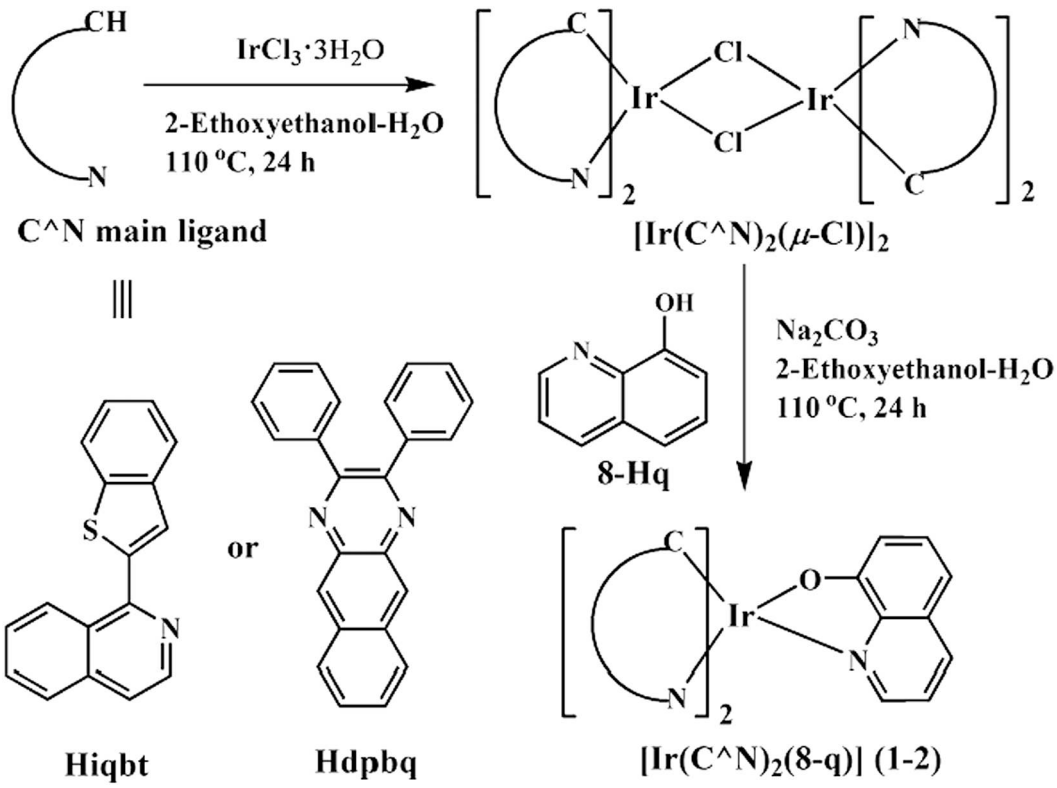

Scheme 1. Reaction scheme for the synthesis of complexes [Ir(iqbt)$_2$(8-q)] (**1**) and [Ir(dpbq)$_2$(8-q)] (**2**).

LEDs), organic-counterparts [7] for NIR organic or polymer light-emitting diodes (NIR-OLEDs or NIR-PLEDs) still dominate in the academic community, which should be arisen from their more versatile and advanced properties in terms of broadened photo- and electro-luminescent spectra as well as endless structure modifications. Moreover, compared with fluorescent small-molecule dyes [8] and conjugated polymers [9] with $^1\pi$-π^*-transitions for NIR luminescence, transition-metal-complex- (Pt(II) or Ir(III)-complex *etc*) [7] and Ln^{3+}-complex-resourced (Ln = Nd, Yb or Er) [10] phosphors are worthy of a particular interest because of their harvesting of both singlet and triplet excitons toward a theoretic 100% internal emission efficiency. Noticeably, in contrast to the narrow-energy-gap-confined [11] rather low NIR quantum efficiency for Ln^{3+}-complex-based (Ln = Nd, Yb or Er) with the emissive wavelength above 900 nm and the notorious efficiency-roll-off [12] inherently contributed from facile aggregation of Pt(II)-centered square-planar system, the compromise of both desirable high-efficiency and low-efficiency-roll-off, to the best of our knowledge, should be expected for iridium(III)-complexes characteristic of typical octahedral configuration and rather short phosphorescent lifetime.

As a matter of fact, from the viewpoint of lowing the emissive energy of iridium(III)-complexes to a restrictive NIR region (700–2500 nm), several approaches have been reported. Utilizing the large π-conjugation porphyrin- [13] or corrole-based [14] macrocycles as the ligands is highly praised at first, since their substantial NIR phosphorescence is commonly originated from the intraligand charge transfer (^{3}ILCT) in the Ir(III)-complexes. However, despite the desirable emission wavelength extended to 800 nm or above for these Ir(III)-complexes, distinctively low NIR quantum efficiencies regulated by energy-gap law [11] actually limit their use for NIR-OLEDs. In contrast, one of the most successful approaches relies on the π-conjugated expansion of the main CˆN-cyclometalated ligand especially incorporated with electron-rich substituents to afford the *fac*-[Ir(CˆN)$_3$]-characteristic homoleptic complex [15] with the expected NIR luminescence ranging at 700–800 nm. Nonetheless, severe aggregation-induced quenching effect from the large π-conjugation of the CˆN main ligand, also makes the molecular design of the *fac*-[Ir(CˆN)$_3$]-complex much challenging in the obtainment of its efficient NIR-OLED or NIR-PLED. Convincingly, significant electronic perturbation can be achieved by modification of the LˆX ancillary ligands [16], from which, the energy gap of its typical [Ir(CˆN)$_2$(LˆX)]-complex is actually adjusted, while bathochromic-shift to effectively narrow the energy gap for NIR luminescence does not have a universal effect. For example, within the typical [Ir(CˆN)$_2$(NˆO)]-complexes with pic as the ancillary ligand, contrast to the rational blue-shift for the well-known Flrpic complex (Flrpic = bis[2-(4,6-difluorophenyl)pyridinato-C^2,N](pic)-iridium(III)) [17], a slight red-shifting [18] at 698 nm for [Ir(iqbt)$_2$(pic)] is realized in relative to that (690 nm) of the *fac*-[Ir(iqbt)$_3$] [19]. Moreover, in consideration of the resolution to [Ir(iqbt)$_2$(pic)] insolubility for solution-processed OLEDs, the success of our reported two [Ir(iqbt)$_2$(NˆO)]-complexes [20] with pic-derived hpa or BF$_2$-hpa as the NˆO ancillary ligand, motivates us a particular concern on the evolution of some other NˆO ancillary ligands. Herein, with 8-hydroxyquinoline (**8-Hq**) as the NˆO ancillary ligand, its two new [Ir(CˆN)$_2$(NˆO)]-heteroleptic complexes with different π-conjugation CˆN main ligands of **Hiqbt** or **Hdpbq** are rationally designed, from which, the desirable red-shifted emission within the NIR regime affected by the electronic perturbations of the CˆN main ligand and the NˆO ancillary ligand are also explored.

The CˆN main ligand **Hiqbt** was synthesized by an improved Suzuki coupling reaction [19] between cost-effective 2-Cl-isoquinoline while not 2-Br-isoquinoline and benzo[*b*]-thien-2-y boronic acid in 73% yield. As to the CˆN main ligand **Hdpbq**, it was obtained from the equimolar condensation of 2,3-naphthalenediamine with benzyl in the presence of oxalic acid according to the well-established procedure from the literature [21]. As shown in Scheme 1, each of the *μ*-chloro-bridged dimmer intermediates **[Ir(iqbt)$_2$(*μ*-Cl)]$_2$** and **[Ir(dpbq)$_2$(*μ*-Cl)]$_2$** were rationally prepared from the reaction of IrCl$_3$·3H$_2$O with the corresponding CˆN main ligand of **Hiqbt** or **Hdpbq**, and used directly for the next step without further purification. Further through the reaction of the NˆO ancillary ligand **8-H*q*** with the corresponding *μ*-chloro-bridged dimmer intermediate **[Ir(iqbt)$_2$(*μ*-Cl)]$_2$** or **[Ir(dpbq)$_2$(*μ*-Cl)]$_2$**, two

Table 1
Photo-physical and electrochemical properties of complexes **1–2** in solution at room temperature.

Complex	Absorption	Emission					Energy level	
	λ_{abs}[a]	λ_{em}[a]	τ[a]	Φ_{em}[a]	k_r[a]	k_{nr}[a]	HOMO[b]	LUMO[b]
	(nm)	(nm)	(μs)		($\times 10^5\ s^{-1}$)	($\times 10^5\ s^{-1}$)	(eV)	(eV)
[Ir(iqbt)$_2$(8-q)] (**1**)	229, 284, 367, 443, 500, 654	687, 756(sh)	0.73	0.16	2.19	1.15	−5.172	−2.662
[Ir(dbpq)$_2$(8-q) (2)] (**2**)	238, 285, 325, 411, 541, 689	786	0.47	0.05	1.06	2.02	−5.148	−3.140

Rate constant *k*r and *k*nr are calculated using the equations $kr = \Phi_{em}/\tau$ and $k_{nr} = (1\text{-}\Phi_{em})/\tau$ on the assumption that $\Phi_{ISC} = 1$ (ISC = intersystem crossing).
[a] In degassed CH_2Cl_2 solution.
[b] HOMO and LUMO levels are obtained from electrochemical determination, respectively.

new Ir(III)-complexes [Ir(iqbt)$_2$(8-q)] (**1**) and [Ir(dpbq)$_2$(8-q)] (**2**) are isolated, respectively.

The two Ir(III)-complexes **1–2** are much soluble in common organic solvents except water, which significantly different from the relative insolubility [Ir(iqbt)$_2$(pic)] [18] while comparable to that of our reported two [Ir(iqbt)$_2$(N^O)]-complexes [20] with pic-derived hpa or BF_2-hpa as the N^O ancillary ligand, renders the incorporation of the **8-Hq** N^O ancillary ligand for its new [Ir(C^N)$_2$(8-q)] complexes (HC^N = **Hiqbt** or **Hdpbq**) an opportunity to solution-processed electro-luminescent devices. Moreover, Ir(III)-complexes **1–2** were well-characterized by EA, FT-IR, ^{1}H NMR and ESI-MS. In the ^{1}H NMR spectrum (Fig. 1S) of complex **1**, the iridium(III)-induced significantly spread shifts of the (**iqbt**)$^-$ or (**dpbq**)$^-$ and (**L^n**)$^-$ combined proton resonances (δ = 9.13–6.39 ppm) relative to those (δ = 8.65–7.43 ppm) of the free **Hiqbt** ligand are observed. Moreover, the proton signals of the (**iqbt**)$^-$ and (**8-q**)$^-$ ligands with a stipulated molar ratio of 2:1 could further confirm the [Ir(iqbt)$_2$(8-q)] (**1**) characteristic of the typical [Ir(C^N)$_2$(N^O)]-heteroleptic complexes [22]. For comparison, despite the similar combination of both the (**dpbq**)$^-$ and (**8-q**)$^-$ proton resonances (also in Fig. 1S) in a 2:1 M ratio for complex **2**, its evident converge (δ = 8.72–6.25 ppm) of the proton signals relative to those (δ = 9.13–6.39 ppm) of complex **1**, should be arisen from the strong current-circular effect with the large π-conjugated (**dpbq**)$^-$ C^N ligand for complex **2** as compared to the (**iqbt**)$^-$ C^N ligand in complex **1**. Furthermore, the ESI-MS spectra of the two iridium(III)-complexes **1–2** exhibit a similar pattern, where a strongest mass peak at *m/z* 858.10 (**1**) or 1000.15 (**2**) assigned to the major species [M + H]$^+$, respectively, indicates that each of the respective heteroleptic [Ir(C^N)$_2$(N^O)] unit retains stable in solution. The thermal stability of the two iridium(III)-complexes **1–2** investigated by thermogravimetric analysis (TGA; Fig. 2S) shows that their decomposition temperatures (T_d, corresponding to 5% weight loss) can be up to 300 °C.

The photo-physical properties of the C^N main ligand **Hiqbt** or **Hdpbq**, the N^O ancillary ligand **8-Hq** and their two Ir(III)-complexes **1–2** in solution were explored using absorption and photo-luminescence spectrometers, and the results are summarized in Table 1 and Figs. 1–2 and 3–5S. In contrast to the strong absorption bands limited to the λ_{abs} < 400 nm range for the ligands **Hiqbt**, **Hdpbq**, and **8-Hq**, as shown in Fig. 1, both complexes **1–2** exhibit significantly broadened UV–visible-NIR absorption spectra: the intense absorption bands below 400 nm assigned to the spin-allowed intra-ligand π-π* transitions; the moderate absorption bands in the 400–600 nm region probably arisen from the mixed ^{3}LC/^{1,3}MLCT (LC = ligand-centered; MLCT = metal-to-ligand charge transfer, d-π*) transitions [20]; and the weak absorption bands (654 nm for complex **1** or 689 nm for complex **2**) extending over 600 nm possibly attributed to the ground-state excitation into the lowest triplet state (S_0 - T_1). Worthy of notice, the low-energy ^{3}LC/^{1,3}MLCT absorption of complex **1** locates at λ_{abs} = 500 nm, which is distinctively blue-shifted by 39 nm relative to that (λ_{abs} = 539 nm) of the parent *fac*-[Ir(iqbt)$_3$] complex [19]. Similarly, an evident blue-shift by 25 nm as compared with the low-energy ^{3}LC/^{1,3}MLCT absorption (λ_{abs} = 525 nm) of complex [Ir(iqbt)$_2$(pic)] [18], should result from the change in N^O-chelate ancillary ligand field strength. As to complex **2** based on the larger π-conjugation C^N ligand **Hdpbq**, besides the decreased Ir(III)-centered d-(t_{2g}) orbital energy (541 nm) relative to that (500 nm) of complex **1**, the lowest-energy absorption edge almost extends to *ca.* 700 nm, indicating that the molecular conjugation is significantly increased for the formation of [Ir(dbpq)$_2$(8-q)] (**2**) in a delocalized state. Upon photo-excitation (λ_{ex} = 387 nm, Fig. 3S), as

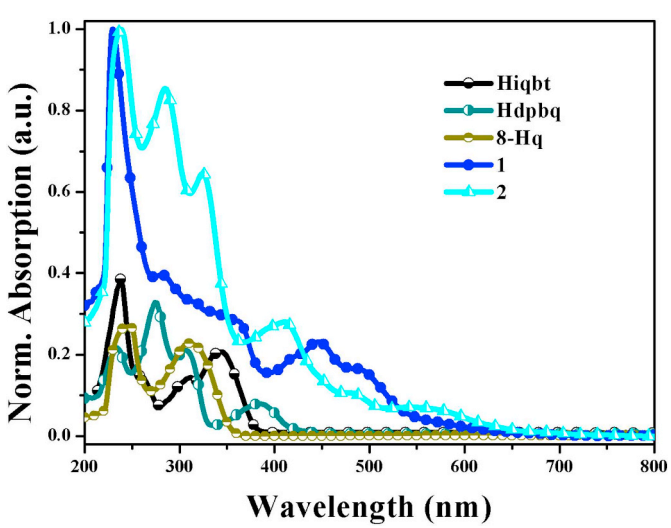

Fig. 1. Normalized UV–Visible-NIR absorption for the Ir(III)-complexes **1–2** in contrast to those of the three ligands **Hiqbt**, **Hdpbq**, **8-Hq** in degassed CH_2Cl_2 solution at RT.

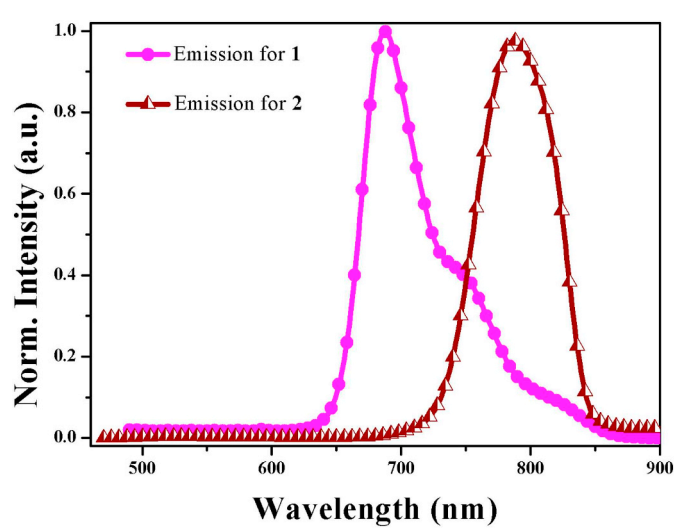

Fig. 2. Normalized NIR photo-luminescence spectra for complexes **1–2** in degassed CH_2Cl_2 solution at RT.

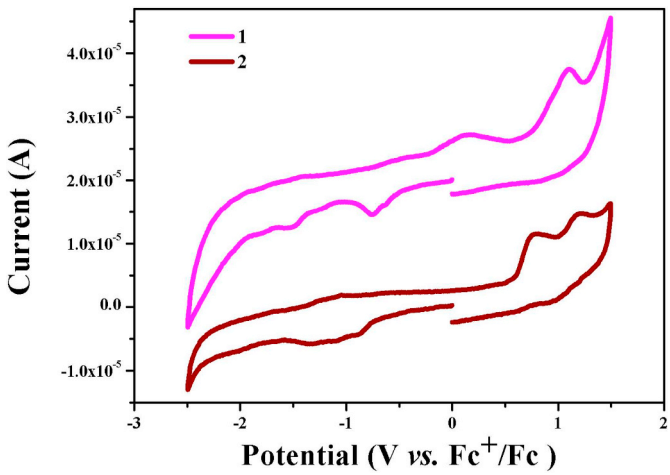

Fig. 3. Cyclic voltammograms of complexes **1–2** recorded *versus* Fc^+/Fc in solution at RT under a N_2 atmosphere (scan rate = 100 mV s^{-1}).

shown in Fig. 2, the strong emission peak (687 nm) of complex **1** lies at the edge of the NIR region besides a shoulder peak at 756 nm. By contrast, complex **2** exhibits a typical NIR luminescence with the emissive wavelength up to 786 nm. Due to the non-emissive character (Fig. 4S) of both the CˆN main ligand **Hiqbt** or **Hdpbq** and the NˆO ancillary ligand **8-Hq** in that NIR region, the NIR emissions of complexes **1–2** should originate from the ligands-perturbed ^{3}LC/^{1,3}MLCT-excited state. Moreover, the NIR emissive nature of the two complexes is characteristic of typical phosphorescence (Fig. 5S), confirming from the substantial τ = 0.73 μs for complex **1** and τ = 0.47 μs for complex **2**, respectively. Worthy of notice, although the desirable bathochromatic shifts of complex **1** at 687 nm relative to those (682–683 nm) [18] of complexes $[Ir(iqbt)_2(N^\wedge N)]^+$ while the slight blue-shifts relative to those of complexes *fac*-$[Ir(iqbt)_3]$ (690 nm) [19], pic-derived $[Ir(iqbt)_2(N^\wedge O)]$ (692–700 nm) [18,20] and $[Ir(iqbt)_2(O^\wedge O)]$ (707–710 nm) [23] are observed, its attractive quantum yield of Φ_{em} = 0.16 endowed by strong ligands-perturbed effect, can be further validated from the considerably high radiative rate constant ($k_r = 2.19 \times 10^5\ s^{-1}$) and the relatively low non-radiative rate constant ($k_{nr} = 1.15 \times 10^5\ s^{-1}$). For comparison, the distinctively low quantum efficiency (Φ_{em} = 0.05) for complex **2** advantageous of a typical NIR (786 nm) phosphorescence, should be regulated from the energy-gap law [11] and also confirmed by its two times smaller k_r of $1.06 \times 10^5\ s^{-1}$ while two times larger k_{nr} of $2.02 \times 10^5\ s^{-1}$ as compared to complex **1**.

For insight into the electronic structures of the two NIR-emissive complexes **1–2**, their electrochemical properties in anhydride MeCN solution were investigated, and the results were summarized in Table 1 and Fig. 3. During the anodic scan shown in Fig. 3, a reversible oxidation process is detected at half-wave potentials of +0.372 and + 0.348 V *versus* Fc^+/Fc for complexes **1–2**, respectively, which should originate from the one-electron oxidation [12] of the Ir(III)-center and the cyclometalated benzo[*b*]thiophene or *benzo[g]quinoxaline* moieties. As compared with complex **1**, the **Hdpbq**-based complex **2** starts to be oxidized at the more positive potential with the shift of 0.024 V, which should reasonably ascribed to its more difficult oxidation due to the stronger π-back-bonding effect from the Ir(III)-center to the CˆN main ligands. Considering no distinctive reduction waving for each of the two Ir(III)-complexes and basing on the reasonable E_g^{OPT} value of 2.07 eV for complex **1** or 1.90 eV for complex **2** estimated from the low-energy absorbance edge (599 nm for complex **1** *versus* 653 nm for complex **2**), the determined HOMO and LUMO levels of −5.172 and − 2.662 eV for complex **1** or − 5.148 and − 3.140 eV for complex **2** are obtained, respectively. In agreement with the E_g^{OPT}-sized trend [20] and the actual bathochromatic shift of complex **2** in comparison with complex **1**, complex **2** exhibits a slightly narrower HOMO-LUMO gap of 2.008 eV than that (2.662 eV) of complex **1**.

In summary, through **Hiqbt** or **Hdpbq** as the CˆN main ligand and **8-Hq** as the NˆO ancillary ligand, two new soluble Ir(III)-complexes $[Ir(iqbt)_2(8\text{-}q)]$ (**1**) and $[Ir(dbpq)_2(8\text{-}q)]$ (**2**) characteristic of a similar $[Ir(C^\wedge N)_2(N^\wedge O)]$-heteroleptic configuration are obtained, respectively. In comparison with the photo-physical property (λ_{em} = 687 nm with a shoulder at 756 nm, lifetime τ = 0.73 μs and quantum efficiency Φ_{em} = 0.16) for complex **1**, complex **2** with large-molecule-conjugation exhibits the distinctive bathochromatic shift into a typical NIR region (λ_{em} = 786 nm), endowing a particular opportunity to future NIR-OLED.

Acknowledgements

This work is funded by the NNSF (21373160 and 21173165) and the Graduate Innovation and Creativity Fund (YZZ17127) of Northwest University in P. R. of China.

Appendix A. Supplementary data

The information of raw materials and methods, and the synthesis and characterization of the two CˆN ligands **Hiqbt** and **Hdpbq**, the two μ-chloro-bridged dimmer intermediates **$[Ir(iqbt)_2(\mu\text{-}Cl)]_2$** and **$[Ir(dpbq)_2(\mu\text{-}Cl)]_2$** and their two Ir(III)-complexes $[Ir(iqbt)_2(8\text{-}q)]$ (**1**) and $[Ir(dpbq)_2(8\text{-}q)]$ (**2**) depicted in the Supporting information. The ^{1}H NMR spectra, the TG curves, the solution visible emission and/or excitation spectra of the ligands **Hiqbt**, **Hdpbq** and **8-Hq** and the two Ir(III)-complexes **1–2** and the time-decayed curves deposited in Figs. 1–4S, respectively. Supplementary data to this article can be found online at https://doi.org/10.1016/j.inoche.2019.01.019.

References

[1] M.F. Harrison, J.P. Neary, W.J. Albert, M.D.W. Veillette, C. Forcest, N.P. McKenzie, J.C. Croll, Physiological effects of night vision goggle counterweights on neck musculature of military helicopter pilots, Mil. Med. 172 (2007) 864–870.
[2] D.J.E. Knight, Laser frequency standards in the near infrared, coinciding with the optical fiber transmission bands, Laser Phys. 4 (1994) 345–348.
[3] X.Y. Yao, C.L. Liu, G. Chen, D.X. Feng, J. Yin, Transcranial near-infrared laser therapy in improving cognitive recovery of function following traumatic brain injury, Curr. Neuropharmacol. 16 (2018) 1320–1326.
[4] T.Q. Wu, N.R. Branda, Using low-energy near infrared light and upconverting nanoparticles to trigger photoreactions within supramolecular assemblies, Chem. Commun. 52 (2016) 8636–8644.
[5] H. Wang, D.H. Kim, Perovskite-based photodetecttors: materials and devices, Chem. Soc. Rev. 46 (2017) 5204–5236.
[6] J. Pichaandi, F.C.J.M. van Veggel, Near-infrared emitting quantum dots: recent progress on their synthesis and characterization, Coord. Chem. Rev. 263-264 (2014) 138–150.
[7] C.-L. Ho, H. Li, W.-Y. Wong, Red to near-infrared organometallic phosphorescent dyes for OLED applications, J. Organomet. Chem. 751 (2014) 261–285.
[8] A. Barbieri, E. Bandini, F. Monti, V.K. Praveen, N. Armaroli, The rise of near-infrared emitters: organic dyes, porphyrinoids, and transition metal complexes, Top. Curr. Chem. 374 (2016) 1–39.
[9] H. Chen, B.L. Dong, Y.H. Tang, W.Y. Lin, A unique "integration" strategy for the rational design of optical tunable near-infrared fluorophore, Acc. Chem. Res. 50 (2017) 1410–1422.
[10] S.V. Eliseeva, J.-C.G. Bünzli, Lanthanide luminescence for functional materials and bio-science, Chem. Soc. Rev. 39 (2010) 189–227.
[11] J. Xue, L. Chen, L.J. Xin, L. Duan, J. Qiao, High-efficiency and low efficiency roll-off near-infrared fluorescent OLEDs through triplet fusion, Chem. Sci. 7 (2016) 2888–2895.
[12] H.F. Xiang, J.H. Cheng, X.F. Ma, X.G. Zhou, J.J. Chruma, Near-infrared phosphorescence: materials and applications, Chem. Soc. Rev. 42 (2013) 6128–6185.
[13] L. Qin, X.G. Guan, Y. Chen, J.S. Huang, C.-M. Che, Near-infrared phosphorescent supramolecular alkyl/aryl-iridium porphyrin assemblies by axial coordination, Chem. Eur. J. 24 (2018) 14400–14408.
[14] J.H. Palmer, A.C. Durrell, Z. Gross, J.R. Winkler, H.B. Gray, J. Am. Chem. Soc. 132 (2010) 9230–9231.
[15] J. Xue, L.J. Xin, J.Y. Hou, L. Duan, R.J. Wang, Y. Wei, J. Qiao, Homoleptic facial Ir(III) complexes via facile synthesis for high-efficiency and low-roll-off near-infrared organic light-emitting diodes over 750 nm, Chem. Mater. 29 (2017) 4775–4782.
[16] A.F. Henwood, E. Zysman-Colman, Lessons learned in tuning the optoelectronic properties of phosphorescent iridium(III) complexes, Chem. Commun. 53 (2017)

807–826.
[17] J. Liu, M.H. Jiang, X.Y. Zhou, C.J. Zhan, J. Bai, M. Xiong, F.F. Li, Y.H. Liu, High-efficient sky-blue and green emissive OLEDs based on Flrpic and FIrdfpic, Synth. Met. 234 (2017) 111–116.
[18] G.N. Li, Y. Zou, Y.D. Yang, J. Liang, F. Cui, T. Zheng, H. Xie, Z.G. Niu, Deep-red phosphorescent iridium(III) complexes containing 1-(benzo[*b*]thiophen-2-yl)isoquinoline ligand: synthesis, photophysical and electrochemical properties and DFT calculations, J. Fluoresc. 24 (2014) 1545–1552.
[19] S. Ikawa, S. Yagi, T. Maeda, H. Nakazumi, H. Fujiwara, S. Koseki, Y. Sakurai, Photo- and electroluminescence from deep-red- and near-infrared-phosphorescent tris-cyclometalated iridium(III) complexes bearing largely π-extended ligands, Inorg. Chem. Commun. 38 (2013) 14–19.
[20] G.R. Fu, H. Zheng, Y.N. He, W.T. Li, X.Q. Lü, H.S. He, Efficient near-infrared (NIR) polymer light-emitting diodes (PLEDs) based on heteroleptic iridium(III) complexes with post-modification effects of intramolecular hydrogen bonding or BF_2-chelation, J. Mater. Chem. C 6 (2018) 10589–10596.
[21] H.-Y. Chen, C.-H. Yang, Y. Chi, Y.-M. Cheng, Y.-S. Yeh, P.-T. Chou, H.-Y. Hsieh, C.-S. Liu, S.-M. Peng, G.-H. Lee, Room-temperature NIR phosphorescence of new iridium (III) complexes with ligands derived from benzoquinoxaline, Can. J. Chem. 84 (2006) 309–318.
[22] T.Y. Li, J. Wu, Z.G. Wu, Y.X. Zheng, J.L. Zuo, Y. Pan, Rational design of phosphorescent iridium(III) complexes for emission color tenability and their applications in OLEDs, Coord. Chem. Rev. 374 (2018) 55–92.
[23] S. Kesarkar, W. Mróz, M. Penconi, M. Pasini, S. Destri, M. Cazzaniga, D. Ceresoli, P.R. Mussini, C. Baldoli, U. Giovanella, A. Bossi, Near-IR emitting iridium(III) complexes with heteroaromatic *β*-diketonate ancillary ligands for efficient solution-processed OLEDs: structure-property correlations, Angew. Chem. Int. Ed. 55 (2016) 2714–2718.